HO-1 knockdown upregulates the expression of VCAM-1 to induce neutrophil recruitment during renal ischemia-reperfusion injury

YECHENG HE[1*], HUADONG LI[2*], JUAN YAO[3*], HUA ZHONG[4], YANBIN KUANG[5], XIN LI[6] and WEIHUA BIAN[7]

[1]Department of Clinical Medicine, Suzhou Vocational Health College, Suzhou, Jiangsu 215009; [2]Department of Cardiovascular Surgery, Union Hospital, Tongji Medical College, Huazhong University of Science and Technology, Wuhan, Hubei 430022; [3]Department of Nursing, Suzhou Vocational Health College, Suzhou, Jiangsu 215009; [4]College of Life Sciences, Wuhan University, Wuhan, Hubei 430072; [5]Department of Respiratory Medicine, Ren Ji Hospital, School of Medicine, Shanghai Jiao Tong University, Shanghai 200123; [6]Key Laboratory of Growth Regulation and Translational Research of Zhejiang Province, School of Life Sciences, Westlake University, Hangzhou, Zhejiang 310024; [7]Department of Cell Biology, Binzhou Medical University, Yantai, Shandong 264003, P.R. China

Received January 16, 2021; Accepted July 14, 2021

DOI: 10.3892/ijmm.2021.5018

Abstract. Heme oxygenase-1 (HO-1) has been reported to be upregulated following renal ischemia-reperfusion injury (IRI) and plays a key cytoprotective role; however, the underlying molecular mechanisms of its protective effects remain poorly understood. In the present study, in order to further elucidate the molecular mechanisms underlying the cytoprotective role of HO-1 in renal IRI, HO-$1^{+/+}$ and HO-$1^{+/-}$ mice were subjected to renal ischemia and subsequent reperfusion followed by the analysis of blood urea nitrogen (BUN) and serum creatinine (SCr) levels, the severity of histological changes, HO-1 and vascular cell adhesion molecule-1 (VCAM-1) protein expression, the mRNA expression of inflammatory factors and the effects of VCAM-1 blockade. The results of the present study demonstrated that the upregulated expression levels of VCAM-1 in HO-$1^{+/-}$ mice during IRI increased the extent of renal tissue damage and activated the inflammatory response. These effects were subsequently reversed following infusion with an anti-VCAM-1 antibody. In addition, the upregulated expression of VCAM-1 in mouse glomerulus vascular endothelial cells isolated from HO-$1^{+/-}$ mice increased the adhesion and migration of neutrophils, effects which were also reversed upon incubation with an anti-VCAM-1 antibody. These results indicated that HO-1 knockdown may upregulate the expression of VCAM-1 during renal IRI, resulting in increased neutrophil recruitment and the activation of the inflammatory response, thereby exacerbating renal IRI. The present study thus highlights the regulatory mechanisms of HO-1 in renal IRI and provides a potential target for the clinical treatment of IRI following renal transplantation.

Correspondence to: Dr Weihua Bian, Department of Cell Biology, Binzhou Medical University, 346 Guanhai Road, Yantai, Shandong 264003, P.R. China
E-mail: bian_1005@163.com

*Contributed equally

Key words: heme oxygenase-1, vascular cell adhesion molecule-1, renal ischemia-reperfusion injury, neutrophil recruitment, adhesion, migration

Introduction

Renal ischemia-reperfusion (IR) injury (IRI) is one of the leading causes of acute kidney injury (AKI), as it causes renal cell dysfunction to varying degrees, which ultimately leads to death (1,2). The increased demand for kidney allografts worldwide suggests that there is an increased risk of developing AKI (3,4). However, there is currently no cure available for renal IRI, at least to the best of our knowledge; therefore, the further exploration of the underlying pathological mechanisms may lead to the development of more effective treatment options and a more successful transplantation rate.

Heme oxygenase (HO) is a rate-limiting enzyme that degrades heme into iron, carbon monoxide and biliverdin (5). In total, three distinct subtypes of the enzyme have been identified: Inducible HO-1, also known as heat shock protein 32, and the constitutively expressed HO-2 and HO-3 (6). The increased expression of HO-1 has been suggested to play a key cytoprotective role in maintaining the redox homeostasis and activating the oxidative stress defense mechanism when cells are subjected to certain types of stress, such as inflammation, ischemia, hypothermia or radiation exposure (7). HO-1 was discovered to be induced in response to renal IRI (8-10), and to prolong renal allograft survival, reduce renal tubular damage induced by IRI and improve renal function (11,12).

However, to the best of our knowledge, the molecular mechanisms through which HO-1 exerts its cytoprotective

effects remain poorly understood. Leukocytes are key players in the immune and inflammatory responses activated following transplantation, and must anchor to vascular endothelial cells (ECs) first to exert their functions (13). ECs are activated in response to inflammatory stimuli through the upregulation of a number of adhesion molecules, such as P-selectin, intracellular adhesion molecular (ICAM)-1 (also known as CD54) and vascular cell adhesion molecule (VCAM)-1 (also known as CD106), which promotes the adhesion, activation and migration of circulating leukocytes (14-17). HO-1 has been found to be one of the principal proteins regulating the expression of adhesion molecules associated with EC activation (18). Previous studies have demonstrated that hemoglobin exposure is able to increase vascular permeability and thereby improve leukocyte infiltration into the spleen, intestine and liver, which is associated with the upregulation of ICAM-1, P-selectin and fibronectin expression (19,20).

VCAM-1 is an important adhesion molecule associated with EC activation (21,22). The induced expression of VCAM-1 has been reported to increase the adhesion of leukocytes expressing the counter receptor, integrin α4β1 (23,24). However, to the best of our knowledge, whether HO-1 affects the recruitment of neutrophils by regulating VCAM-1 expression during renal IRI has not yet been investigated.

The present study thus aimed to investigate the mechanisms through which HO-1 regulates the recruitment of neutrophils in renal IRI. The present study used HO-1 knockdown ($HO\text{-}1^{+/-}$) mice, rather than HO knockout ($HO\text{-}1^{-/-}$) mice, as the animal model since a partial reduction in HO-1 levels is more common and clinically relevant than the complete elimination of HO-1, and $HO\text{-}1^{-/-}$ mice also have a high mortality rate (25). The present study reveals a protective role of HO-1 in renal IRI by regulating VCAM-1 expression. It is possible to explore some treatment methods through this target in the future.

Materials and methods

Genotype identification of mice. $HO\text{-}1^{+/-}$ and wild-type ($HO\text{-}1^{+/+}$) mice (n=7 in each group) were provided by Jackson Laboratory. DNA from mouse tail tips were extracted using a Genomic DNA Extraction kit from Accurate Biotechnology Co., Ltd. (cat. no. AG21009). The DNA was used as a template to perform the PCR assay. PCR was performed with 10 μl Taq 2X PCR master mix (K0171, Thermo Fisher Scientific, Inc.), 2 μl mixed primers (10 μM of primer each), 1 μl genomic DNA and 7 μl ddH_2O. Target DNA was amplified in a thermocycler machine (ABI Veriti), with initial denaturation at 95˚C for 5 min, followed by 35 cycles of denaturation at 95˚C for 20 sec, annealing at 58˚C for 30 sec, and extension at 72˚C for 30 sec. The PCR products were electrophoresed on a 2% TBE Agarose gel and imaged in a Gel Imaging System (Tanon 2500, Tanon Science & Technology Co., Ltd.). Primers P1 (GTACATGCTGGCTGGGTTCT), P2 (CCATTTCTCAGG CAAGAAGG) and P3 (GCCAGAGGCCACTTGTGTAG) were used to identify $HO\text{-}1^{+/+}$ [size, 280 base pair (bp)] and $HO\text{-}1^{+/-}$ (size, 280 and 225 bp) mice.

Renal ischemia reperfusion model. All mice were housed under specific pathogen-free conditions in strict compliance with the facility standards approved by the China Laboratory Animal Management Accreditation Association. All experiments performed in the study were approved by the Institutional Animal Care and Use Committee of Binzhou Medical University (PJ2018-10-16). $HO\text{-}1^{+/+}$ and $HO\text{-}1^{+/-}$ mice were anesthetized by an inhalation of isoflurane (5% for induction and 2% for maintenance). The hair on the backs of each mouse was partially removed using hair removal cream and the exposed skin was disinfected with 75% alcohol; the mice were then fixed on a 37˚C thermostat (heating pad) in the prone position. A midline incision was made, the vessels of the bilateral renal pedicles were exposed, and the right renal artery was clamped using a non-traumatic vascular clamp (size B-1 V; S&T AG-Microsurgical Instruments) for 60 min. After the midline incision was made, the vessels of the bilateral renal pedicles were exposed and the right renal artery was clamped using a temporary clip (Serrefine Vascular Clamps, MDG0795861; Medline) for 60 min. During the clamping process, the color of the kidney changed from bright red to purple/black. After 60 min, the renal artery clip was released to initiate blood flow reperfusion. Furthermore, to prevent functional compensation by the left kidney, it was removed following left renal pedicle ligation. After the wound was sutured, the mice were woken and returned to a clean cage to recover from the anesthetic.

In vivo blocking experiment. A total of 30 male mice were randomly divided into the following 3 groups (n=10/group): i) The $HO\text{-}1^{+/-}$ group; ii) $HO\text{-}1^{+/+}$ group; and iii) the $HO\text{-}1^{+/-}$ + anti-VCAM-1 antibody group. Prior to renal IR surgery, the animals were administered mouse anti-VCAM-1 monoclonal antibody (cat. no. AF643; R&D Systems, Inc.) at 1 mg/kg through the tail vein, which was set as the trial dose (26).

The control animals were injected with equal amounts of isotype-matched antibodies (1 mg/kg, cat. no. MAB002; R&D Systems, Inc.). Each animal received the same dose of monoclonal antibody injection at 24, 48 and 72 h after surgery. At the end of the monoclonal antibody treatment, the animals were anesthetized with 5% inhaled isoflurane for induction and 2% for maintenance, the kidneys were harvested, and the mice were immediately euthanized by cervical dislocation.

Western blot analysis. The mouse kidney tissue was lysed with Protein Extraction Reagent (cat. no. 78505; Thermo Fisher Scientific, Inc.) containing protease-inhibitor (cat. no. P8340, Sigma-Aldrich; Merck KGaA) and the protein concentration was quantified using a BCA protein assay kit (Beijing Solarbio Science & Technology Co., Ltd.) and 30 μg protein from each group was separated via 10% SDS-PAGE. The separated proteins were subsequently transferred onto a polyvinylidene fluoride membrane and blocked with 5% milk for 1 h. The membranes were then incubated with the following primary antibodies overnight at 4˚C: Anti-VCAM-1 (0.25 μg/ml, cat. no. AF643; R&D systems), anti-HO-1 (1:1,000, cat. no. 27282-1-AP; ProteinTech Group, Inc.), anti-cleaved caspase-3 (1:1,000, cat. no. 9664; Cell Signaling Technology, Inc.) and anti-β-actin (1:1,000, cat. no. 58169; Cell Signaling Technology, Inc.), followed by the horseradish

peroxidase-conjugated anti-goat (1:2,000, cat. no. ab97110; Abcam), anti-rabbit (1:2,000, cat. no. 7074; Cell Signaling Technology, Inc.) or anti-mouse secondary antibodies (1:2,000, cat. no. 7076; Cell Signaling Technology, Inc.) at room temperature for 1 h. Protein bands were visualized using an ECL reagent (Beyotime Institute of Biotechnology) and analyzed using densitometry with ImageJ software (version 1.48; National Institutes of Health).

Determination of histological scores. After the mice were sacrificed, the kidneys were immediately fixed with 4% paraformaldehyde for 24 h and embedded in paraffin according to the standard protocol as previously described (27). The kidneys were then sectioned into 5-μm-thick slices using a paraffin microtome (Leica RM CoolClamp; Leica Microsystems, Inc.). Hematoxylin and eosin (H&E) staining was performed according to the standard protocol as previously described (28,29). To quantify the extent of tubular injury, the H&E-stained sections were visualized under a light microscope (Olympus IX83; Olympus Corporation) and the degree of tubular injury was scored using a five-point scale, based on the following criteria: 0, normal tubule; 1, slight blistering and loss of brush borders; 2, severe blistering and mild vacuolization; 3, significant vacuolization and shrunken nuclei; 4, presence of necrotic or apoptotic cells and denudation of the basement membrane; and 5, complete tubular necrosis (30).

Determination of renal function. To evaluate the changes in renal function following renal I/R surgery, the $HO^{+/+}$ and $HO\text{-}1^{+/-}$ mice were sacrificed at 8, 24 and 72 h post-reperfusion, and 200 μl of blood were collected from the dorsal aorta into heparinized Eppendorf tubes as previously described (31). The blood was left to clot in an upright position for 30 min and then centrifuged for 15 min at 1,480 x g at 4˚C, then serum was obtained for the measurement of blood urea nitrogen (BUN) and serum creatinine (SCr) levels (28). The concentrations of SCr (mg/dl) and BUN (mg/dl) were measured using a Cobas Fara spectrophotometer system (UV-7504; Roche Diagnostics).

Reverse transcription-quantitative PCR (RT-qPCR). Total RNA from the mouse kidneys was extracted using TRIzol® reagent and reverse transcribed into cDNA using a SuperScript III First-Strand synthesis kit (18080051, Invitrogen; Thermo Fisher Scientific, Inc.). qPCR to determine the mRNA expression levels of IFN-γ, IL-6, TNF-α, IL-10 and MMP-13 was subsequently performed using a SYBR-Green PCR master mix (Applied Biosystems; Thermo Fisher Scientific, Inc.). The relative mRNA expression levels were calculated using the $2^{-\Delta\Delta Cq}$ method and GAPDH was used as the endogenous control for normalization (32). The primer sequences used for qPCR are listed in Table I.

Mouse glomerular EC (mGEC) culture. The mice were anesthetized with 5% inhaled isoflurane for induction and 2% for maintenance and disinfected with 75% alcohol, and placed on a clean hood. The chest was opened for bloodletting from the heart, followed by the opening of the abdominal cavity and the removal of the kidneys. The kidneys were placed in PBS at 4˚C and the renal capsule and medulla were removed; the kidney cortex was then collected and cut into small (1 mm^3) sections. After washing three times with cold PBS, the sections were further homogenized into a slurry and digested with 0.1% type IV collagenase (HBSS dilution) at 37˚C for 25-30 min, which was terminated when the glomerulus was slightly broken and loosened. The renal cortex tissue mass was poured into a stainless steel 200 wire mesh (1985-00200, Bellco), gently grinded and washed repeatedly with PBS at 4˚C to collect the suspension. The latter was poured onto a 400 mesh screen (1985-00400; Bellco) and thoroughly rinsed with PBS at 4˚C so that the kidney tubules and cell debris were filtered out and the glomerulus remained on the 400 mesh screen for collection. The glomerular suspension was centrifuged at 120 x g for 5 min at room temperature, resuspended in endothelial cell culture medium (DMEM plus 20% FBS, L-glutamine 30 μg/ml, bovine insulin 0.6 U/ml, heparin 5 U/ml, penicillin 100 U/ml), and placed in an incubator at 37˚C for 3 days without disturbance. The ECs were allowed to grow out from the adherent glomeruli until 80-90% confluency and passaged with 0.25% trypsin. Cells of two to three generations were used in the subsequent experiments.

Table I. Cytokine-specific primer pair sequences used for RT-qPCR.

Gene name	Primer sequences
IFN-γ	F: AGCGGCTGACTGAACTCAGATTGTAG
IFN-γ	R: GTCACAGTTTTCAGCTGTATAGGG
IL-6	F: CTGGTGACAACCACGGCCTTCCCTA
IL-6	R: ATGCTTAGGCATAACGCACTAGGTT
TNF-α	F: GGCAGGTCTACTTTGGAGTCATTGC
TNF-α	R: ACATTCGAGGCTCCAGTGAATTCGG
IL-10	F: ACCTGGTAGAAGTGATGCCCCAGGCA
IL-10	R: CTATGCAGTTGATGAAGATGTCAAA
MMP-13	F: GATGATCCCACCTTAGACATCATGAGAAAA
MMP-13	R: AAAGTGGTCTTAGATACTACCGTGACG

RT-qPCR, reverse transcription-quantitative PCR; F, forward; R, reverse.

Immunohistochemistry. Immunohistochemical staining of the paraffin-embedded tissues was performed as follows: Following deparaffinization and antigen retrieval, the kidney tissue sections were blocked with 10% goat serum for 1 h and then incubated overnight at 4˚C with the following antibodies: Anti-CD68 antibody (1:100, cat. no. ab283654; Abcam) and anti-lymphocyte antigen 6 complex, locus G (Ly-6G) (1:200, ab25377; Abcam). The following day, following incubation with HRP-conjugated secondary antibodies (1:500, cat. no. ab97057; Abcam; 1:500, cat. no. 7074, Cell Signaling Technology, Inc.) for 1 h at room temperature, the slides were developed with DAB until the signal clearly appeared, and the nuclei were stained with hematoxylin for 5 min at room temperature, and images were obtained using a microscope (Olympus IX83, Olympus Corporation).

TUNEL staining. TUNEL staining was performed using an *In Situ* Cell Death Detection kit (cat. no. 12156792910, Sigma-Aldrich Merck KGaA) according to the manufacturer's instructions on cryosections. Briefly, the sections were washed with PBS and permeabilized with 0.1% Triton X-100 + 0.1% sodium citrate on ice for 5 min. The TUNEL reaction mixture was then added to the tissue followed by incubation at 37˚C for 1 h. Following rinsing three times with PBS, the tissues were mounted with mounting media containing DAPI (cat. no. H-1200; Vector Laboratories, Inc., part of Maravai LifeSciences) and visualized using a fluorescence microscope (Olympus IX83; Olympus Corporation).

Neutrophil purification. Mouse neutrophils were extracted using a peripheral blood Neutrophil isolation kit (cat. no. LZS1100, TBD Hao Yang Biological Manufacture Co., Ltd.). The blood samples were carefully sucked through a straw and added to the surface of the separation solution. Following centrifugation for 30 min at 400 x g and 4˚C, the neutrophil layer was carefully absorbed and the red blood cells were lysed with lysis buffer. After washing, neutrophils were resuspended in DMEM at a concentration of $1x10^6$ cells/ml. Neutrophils were labeled with PKH26 (cat. no. PKH26GL, Sigma-Aldrich; Merck KGaA) to prepare for the adhesion and Transwell migration assays.

Neutrophil adhesion assay. mGECs were grown to confluency in a 96-well plate. Confluent cells were stimulated with 100 U/ml TNF-α (Millipore Sigma) for 4 h. The medium was then replaced with fresh medium and supplemented with 10 μg/ml VCAM-1 (cat. no. AF643; R&D systems) or isotype Mb (cat. no. AB-108-C; R&D systems) for 1 h. Neutrophils labeled with PKH26 were then added to the 96-well plate for 6 h. The cells were then washed with PBS three times and photographed using a fluorescence microscope (Olympus IX83; Olympus Corporation). ImageJ software (version 1.48; National Institutes of Health) was used to quantify the fluorescence area.

Neutrophil Transwell migration assay. A transwell assay was used to detect neutrophil migration through the mGECs. mGECs were grown to confluency on transwells with 12-μm pores. Confluent cells were stimulated with 100 U/ml TNF-α (Millipore Sigma) for 4 h. The medium was then replaced with fresh medium and supplemented with 10 μg/ml VCAM-1 or isotype Mb for 1 h. A neutrophil migration assay was performed as previously described (33). Fluorescently-stained neutrophils ($3x10^4$) were added to the upper chamber for 6 h. The culture medium was aspirated, the upper chamber was removed and the membrane was gently wiped with a paper towel. The membrane was then fixed with 4% PFA for 10 min, washed twice with PBST and images were captured using an Olympus IX83 fluorescence microscope (Olympus Corporation).

Statistical analysis. The IBM SPSS 22 version program was used for analysis. An unpaired t-test and one-way ANOVA were used to analyze the data. The results are expressed as the mean ± SD. $P<0.05$ was considered to indicate a statistically significant difference.

Results

$HO\text{-}1^{+/-}$ knockdown mice exhibit elevated expression levels of VCAM-1 without changes in renal structure and function. Genotypes of $HO^{+/+}$ and $HO^{+/-}$ mice were first identified. As illustrated in Fig. 1A, by agarose gel electrophoresis, the PCR products in the $HO^{+/+}$ group produced a band of 280 bp, and those in the $HO^{+/-}$ group produced two bands of 225 and 280 bp, which suggested that the genotypes of the $HO^{+/+}$ and $HO^{+/-}$ mice were correct. Western blot analysis was used to compare VCAM-1 protein expression in the $HO\text{-}1^{+/-}$ knockdown and wild-type mice. As shown in Fig. 1B-D, HO-1 expression in the $HO\text{-}1^{+/-}$ mice was decreased by 38% relative to that in the wild-type mice, while the expression of VCAM-1 was increased 2.62-fold ($P<0.05$). Furthermore, immunohistochemical staining revealed that VCAM-1 was expressed at a high level in the $HO\text{-}1^{+/-}$ group, while its expression was relatively low in the $HO\text{-}1^{+/+}$ group (Fig. 1E). These results revealed a significant increase in VCAM-1 expression and a decrease in that of HO-1 in the $HO\text{-}1^{+/-}$ mice. In addition, H&E staining was used to detect renal tissue morphology in the $HO\text{-}1^{+/+}$ and $HO^{+/-}$ mice. As shown in Fig. 1F and G, no marked differences were observed in renal tissue morphology and the tubular injury score between the $HO\text{-}1^{+/+}$ and $HO^{+/-}$ group. The BUN and SCr levels were then analyzed to assess renal function. As shown in Fig. 1H and I, no significant differences were observed in the BUN and SCr levels between the $HO\text{-}1^{+/+}$ and $HO^{+/-}$ groups.

Exacerbation of renal IRI in $HO\text{-}1^{+/-}$ mice. To examine the role of HO-1 in the development of AKI, a model of renal IRI was established by clamping the right renal artery for 60 min and blocking left kidney function in the $HO\text{-}1^{+/-}$ and wild-type mice. Right renal tissues and blood were then harvested for analysis at 8, 24 and 72 h following surgery (Fig. 2A). As shown in Fig. 2B and C, HO-1 expression in the $HO\text{-}1^{+/-}$ mice was decreased significantly at 24 h following surgery ($P<0.05$). However, the expression of VCAM-1 and cleaved caspase-3 was significantly increased ($P<0.05$). Immunofluorescence staining was further used to assess the expression of VCAM-1. Higher expression levels of VCAM-1 were observed in the $HO\text{-}1^{+/-}$ mice than in the $HO\text{-}1^{+/+}$ control group (Fig. 2D). H&E staining of the kidney tissue also revealed more tissue damage in the $HO\text{-}1^{+/-}$ mice than in the wild-type mice. In either the cortex or medulla, cell necrosis, brush border loss, cast formation and tubular dilation were more evident in the $HO\text{-}1^{+/-}$ group (Fig. 2E). A substantial increase in the tubular injury score was observed in the $HO\text{-}1^{+/-}$ group. Over time, the tubular injury score changed, increasing during the early time period, peaking at 24 h, and gradually decreasing thereafter (Fig. 2F). The BUN and SCr concentrations were also analyzed to assess renal function. Similar to the tubular injury score, both the BUN and SCr levels were higher in the $HO\text{-}1^{+/-}$ knockdown group, exhibiting maximal values at 24 h (Fig. 2G and H). As shown in Fig. 2G, the BUN level in the $HO\text{-}1^{+/+}$ group was 53 mg/dl at 8 h post-IRI, increased to 110 mg/dl at 24 h and then decreased to 82 mg/dl at 72 h. By contrast, the BUN levels in the $HO\text{-}1^{+/-}$ experimental group were 82 mg/dl at 8 h post-IRI, increased to 191 mg/dl at 24 h and then decreased to 139 mg/dl at 72 h. Compared with the $HO\text{-}1^{+/+}$ control group,

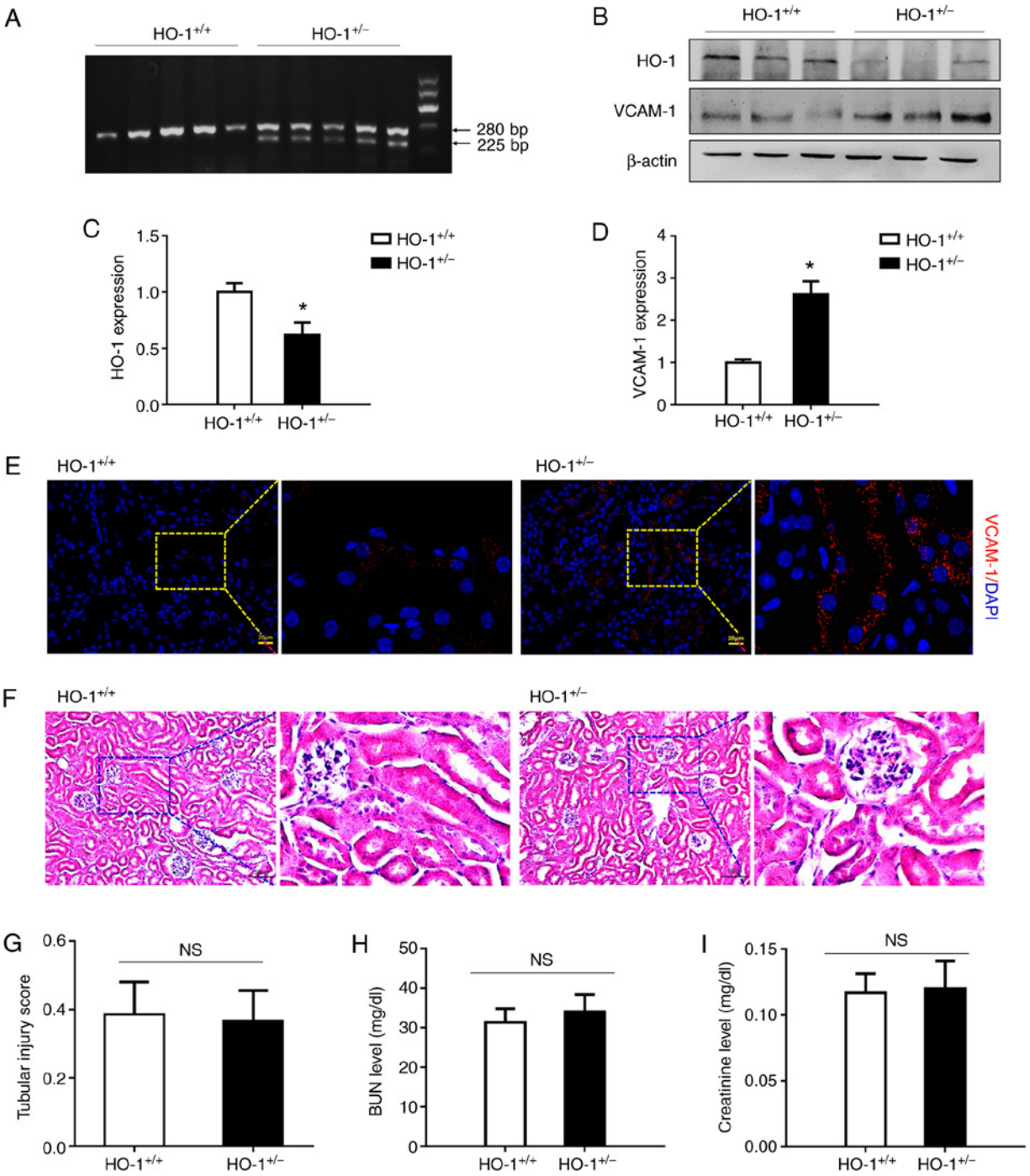

Figure 1. HO-1$^{+/-}$ knockdown mice exhibit elevated expression levels of VCAM-1 without changes in renal structure and function. (A) Genotype identification of HO$^{+/+}$ and HO$^{+/-}$ mice by agarose gel electrophoresis. (B) Western blot analysis of the expression levels of HO-1, VCAM-1 and β-actin proteins in the HO-1$^{+/-}$ vs. those in the wild-type mice. (C and D) Densitometric-based quantification of the western blot analysis results shown in panel B for (C) HO-1 and (D) VCAM-1 proteins using ImageJ software. Densitometry values are expressed as the mean ± SD (n=3). *P<0.05 vs. HO-1$^{+/+}$. (E) Immunohistochemical staining of VCAM-1-expressing cells in the kidneys of the HO-1$^{+/+}$ and HO-1$^{+/-}$ mice. (F) Representative images of H&E-stained sections of renal tissue in the HO-1$^{+/+}$ and HO-1$^{+/-}$ mice. (G) Tissue injury was assessed by using the scoring scale from 0 to 5 points (n=3). (H) Serum creatinine concentration in the HO-1$^{+/+}$ and HO-1$^{+/-}$ mice (n=3). (I) Serum BUN concentration in the HO-1$^{+/+}$ and HO-1$^{+/-}$ mice (n=3). HO-1, heme oxygenase-1; VCAM-1, vascular cell adhesion molecule-1; BUN, blood urea nitrogen.

the BUN levels in the HO-1$^{+/-}$ group were elevated at various time points (P<0.05). As shown in Fig. 2H, in the HO-1$^{+/+}$ group, the SCr level was 0.6 mg/dl at 8 h post-IRI, increased to 1.1 mg/dl at 24 h and then decreased to 0.9 mg/dl at 72 h. However, in the HO-1$^{+/-}$ group, the SCr level was 0.9 mg/dl at 8 h post-IRI, increased to 1.5 mg/dl at 24 h and decreased to 1.2 mg/dl at 72 h. Compared with the HO-1$^{+/+}$ control group, the SCr levels in the HO-1$^{+/-}$ group were elevated at different time points (P<0.05).

IRI can cause an inflammatory response. In order to determine the effects of HO-1 knockdown on the inflammatory response, the expression of inflammatory factors in the injured kidney tissue were analyzed at 24 h post-IRI.

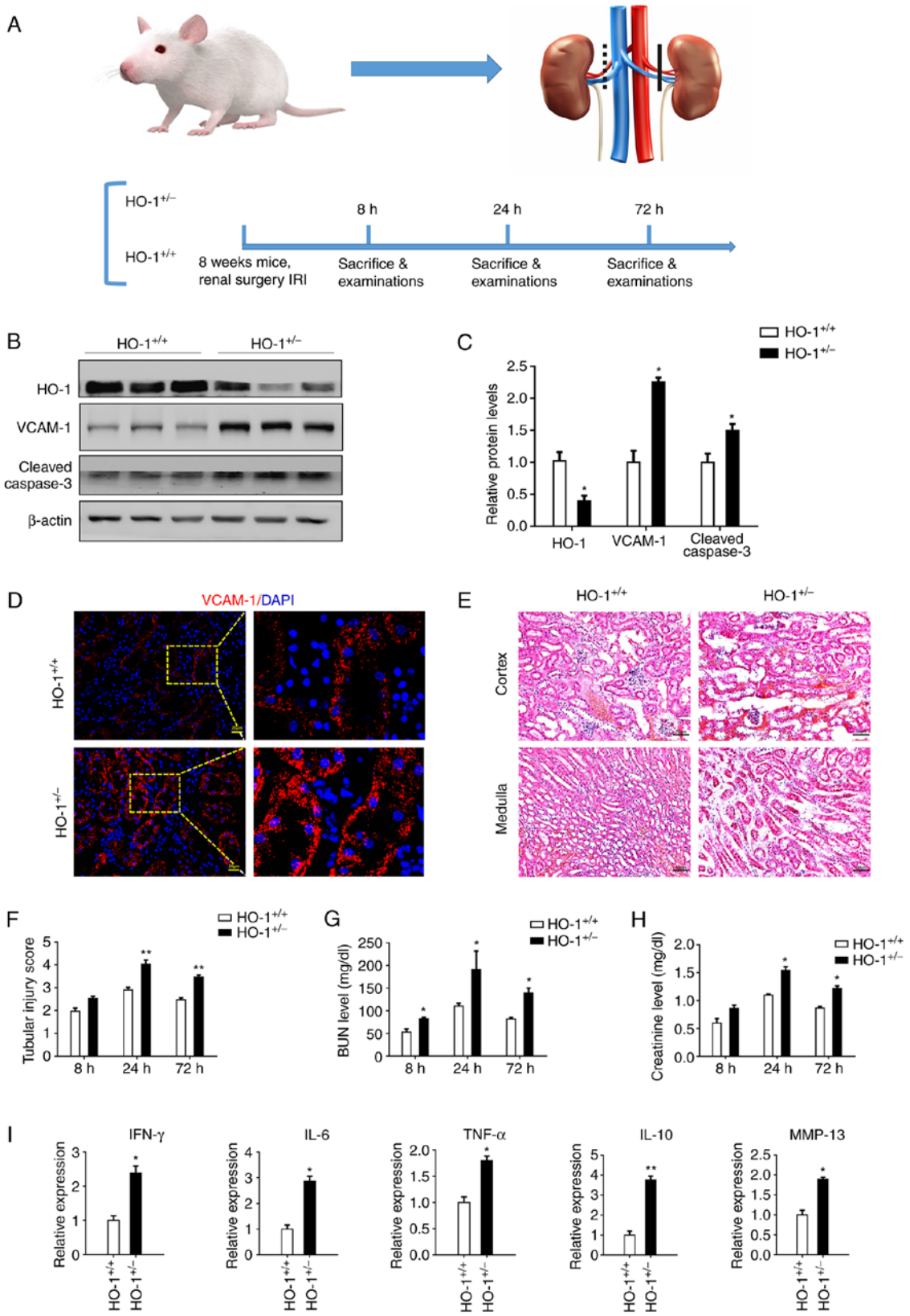

Figure 2. Exacerbation of renal IRI in the HO-1$^{+/-}$ mice. (A) Renal ischemia reperfusion model were established by clamping the right renal artery for 60 min and blocking left kidney function in the HO-1$^{+/-}$, as well as the wild-type mice and tissue harvesting at 8, 24 and 72 h following surgery. (B) Western blot analysis of the expression levels of HO-1, VCAM-1, cleaved caspase-3 and β-actin proteins at 24 h post-IRI in the HO-1$^{+/-}$ vs. those in the wild-type mice. (C) Densitometric-based quantification of the western blot analysis results shown in panel B using ImageJ software. Densitometry values are expressed as the mean ± SD (n=3). *P<0.05 vs. HO-1$^{+/+}$. (D) Immunohistochemical staining of VCAM-1-expressing cells at 24 h post-IRI in the HO-1$^{+/+}$ and HO-1$^{+/-}$ mice. (E) Representative images of H&E-stained sections of the cortical and medullary renal tissue showing the structure of the renal tissue. (F) Tissue injury was assessed by using the scoring scale from 0 to 5 points (n=3, **P<0.01 vs. HO-1$^{+/+}$). (G) Serum BUN concentration at 8, 24 and 72 h post-IRI in the HO-1$^{+/+}$ and HO-1$^{+/-}$ mice (n=3, *P<0.05 vs. HO-1$^{+/+}$). (H) Serum creatinine concentration at 8, 24 and 72 post-IRI in the HO-1$^{+/+}$ and HO-1$^{+/-}$ mice (n=3, *P<0.05 vs. HO-1$^{+/+}$). (I) Expression levels of IFN-γ, IL-6, TNF-α, IL-10 and MMP-13 in the HO-1$^{+/+}$ vs. the HO-1$^{+/-}$ group assessed by RT-qPCR (n=3, *P<0.05, **P<0.01 vs. HO-1$^{+/+}$). IRI, ischemia-reperfusion injury; HO-1, heme oxygenase-1; VCAM-1, vascular cell adhesion molecule-1; BUN, blood urea nitrogen.

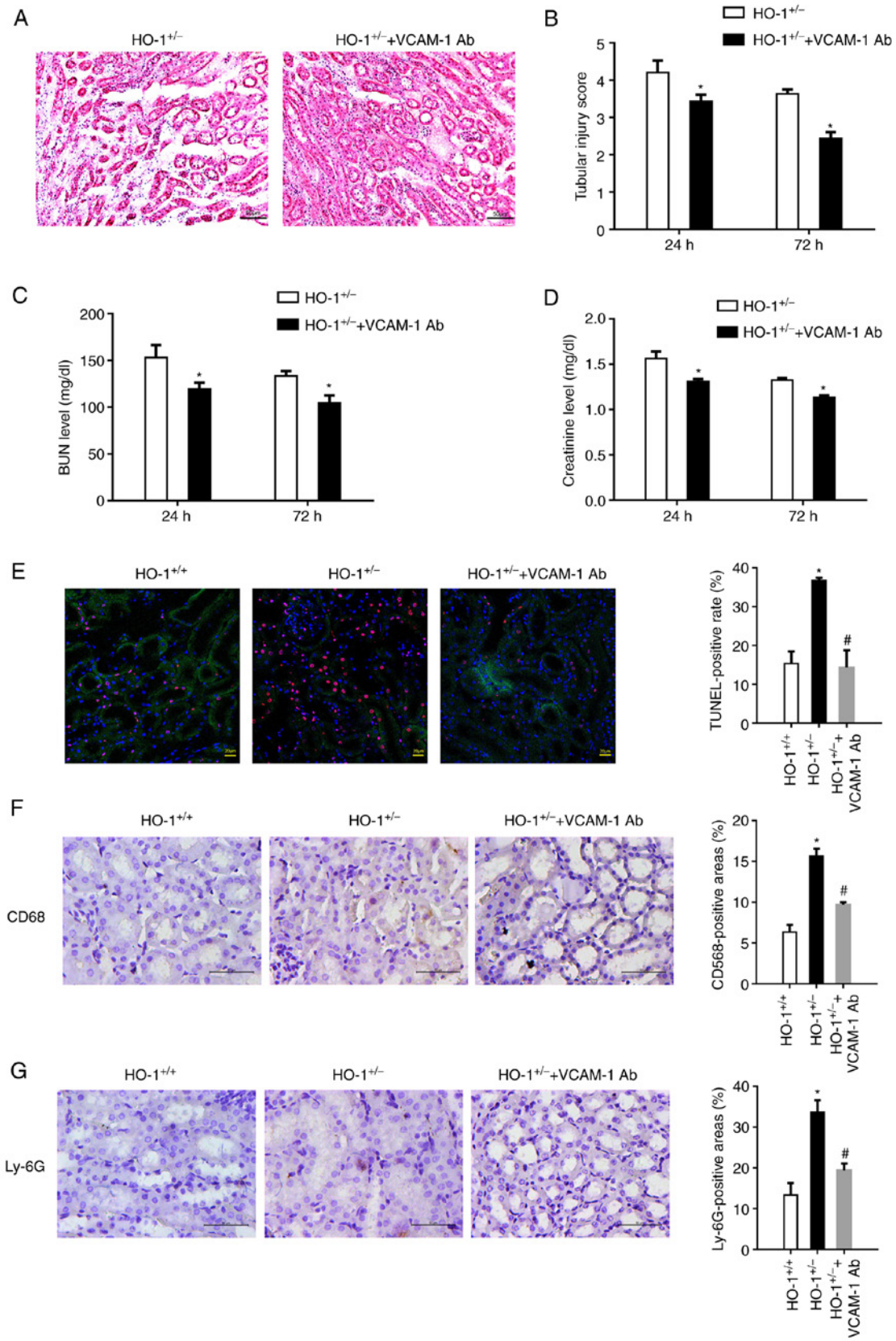

Figure 3. VCAM-1 blocking alleviates renal IRI. VCAM-1 antibody was infused into the HO-1$^{+/-}$ knockdown mice through the tail vein to block VCAM-1 expression on the vascular endothelium. (A) Representative images of H&E-stained sections of renal tissue showing its morphology. (B) Extent of the kidney tissue injury was assessed using the 0 to 5-point scoring system (n=3, *P<0.05 vs. HO-1$^{+/-}$). (C) Serum BUN concentration at 24 and 72 h post-IRI in the HO-1$^{+/+}$ and HO-1$^{+/-}$ mice (n=3, *P<0.05 vs. HO-1$^{+/-}$). (D) Serum creatinine concentration at 24 and 72 h post-IRI in the HO-1$^{+/+}$ and HO-1$^{+/-}$ mice (n=3, *P<0.05 vs. HO-1$^{+/-}$). (E) Cell death upon IRI was measured using TUNEL assay. The TUNEL-positive rate was analyzed using ImageJ software in the HO-1$^{+/+}$, HO-1$^{+/-}$ and HO-1$^{+/-}$ + VCAM-1 Ab groups (*P<0.05 vs. HO-1$^{+/+}$; $^{\#}$P<0.05 vs. HO-1$^{+/-}$). (F) Immunohistochemical staining and quantification analysis of CD68-expressing cells in mouse kidneys in the HO-1$^{+/+}$, HO-1$^{+/-}$ and HO-1$^{+/-}$ + VCAM-1 Ab groups (*P<0.05 vs. HO-1$^{+/+}$; $^{\#}$P<0.05 vs. HO-1$^{+/-}$). (G) Immunohistochemical staining and quantification of Ly-6G-expressing cells in mouse kidneys of the HO-1$^{+/+}$, HO-1$^{+/-}$ and HO-1$^{+/-}$ + VCAM-1 Ab groups (*P<0.05 vs. HO-1$^{+/+}$; $^{\#}$P<0.05 vs. HO-1$^{+/-}$). IRI, ischemia-reperfusion injury; HO-1, heme oxygenase-1; VCAM-1, vascular cell adhesion molecule-1; BUN, blood urea nitrogen; Ab, antibody.

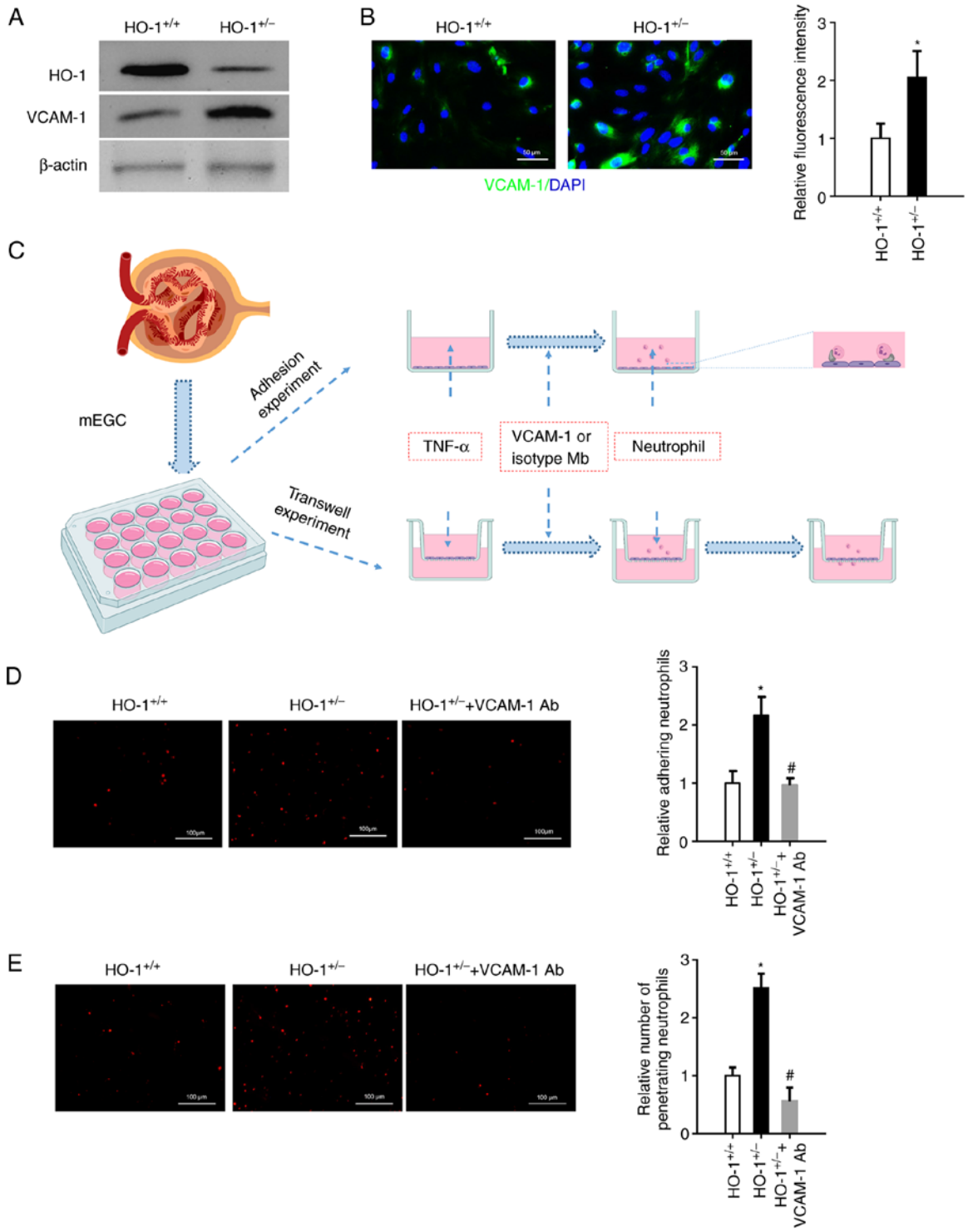

Figure 4. *In vitro* blocking of VCAM-1 suppresses neutrophil adhesion and migration through Transwells. mGECs from the HO-1$^{+/-}$ and wild-type mice were isolated. (A) Western blot analysis of the expression levels of HO-1, VCAM-1 and β-actin proteins in the mGECs extracted from the HO-1$^{+/+}$ and HO-1$^{+/-}$ mice. (B) Immunofluorescence staining of VCAM-1 in the mGECs extracted from the HO-1$^{+/+}$ and HO-1$^{+/-}$ mice. Relative fluorescent intensity was quantified using ImageJ software (n=3, *P<0.05 vs. HO-1$^{+/+}$). (C) mGECs were grown in a 96-well plate or Transwell chamber and stimulated with 100 U/ml TNF-α for 4 h. Neutrophils were isolated and labeled with PKH26 to perform adhesion assay or Transwell migration assay. (D) Neutrophils adhered to mGECs were photographed using a fluorescence microscope, and the fluorescence area was quantified using ImageJ software (n=3, *P<0.05 vs. HO-1$^{+/+}$; $^{\#}$P<0.05 vs. HO-1$^{+/-}$). (E) Neutrophil migration through mGECs was photographed using a fluorescence microscope, and the fluorescence area was quantified using ImageJ software (n=3, *P<0.05 vs. HO-1$^{+/+}$; $^{\#}$P<0.05 vs. HO-1$^{+/-}$). mGECs, mouse glomerular endothelial cells; HO-1, heme oxygenase-1; VCAM-1, vascular cell adhesion molecule-1; Ab, antibody.

The expression levels of IFN-γ, IL-6, TNF-α, IL-10 and MMP-13 in the HO-1$^{+/-}$ group were 2.4-, 2.9-, 1.8-, 3.8- and 1.9-fold higher relative to those in the HO-1$^{+/+}$ group, respectively (Fig. 2I). All these factors exhibited elevated expression levels in the HO-1$^{+/-}$ group, as compared with the HO-1$^{+/+}$ group.

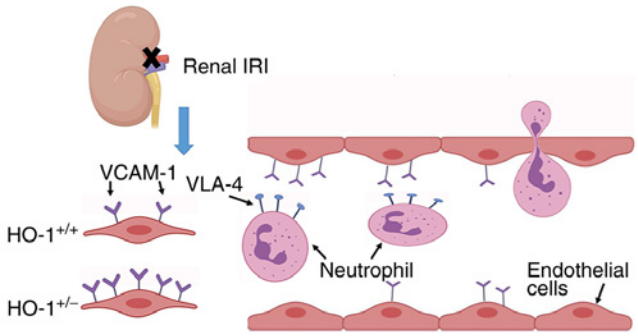

Figure 5. Schematic representation of the proposed mechanisms. Neutrophils bind to mGECs through the interaction of VLA-4 and VCAM-1 to activate mGECs. The expression level of VCAM-1 in HO-1$^{+/-}$ knockdown mice is elevated, resulting in excessive neutrophil adhesion and migration through mEGCs, and eventually exacerbating renal IRI. mGECs, mouse glomerular endothelial cells; HO-1, heme oxygenase-1; VLA-4, very late antigen 4; VCAM-1, vascular cell adhesion molecule-1; IRI, ischemia-reperfusion injury.

VCAM-1 blocking alleviates renal IRI. VCAM-1 antibody was infused into the HO-1$^{+/-}$ mice to block VCAM-1 expression on the inner vascular endothelium. Tubular injury was found to be visibly reduced in the VCAM-1 antibody infusion group (Fig. 3A). The estimated histopathological scoring also suggested alleviated tubular injury in the HO-1$^{+/-}$ knockdown mice upon VCAM-1 blocking (Fig. 3B). In addition, the BUN and SCr levels were measured to assess kidney functionality. As shown in Fig. 3C, at 24 h post-IRI, the BUN concentration value was 156.3±18.6 mg/dl in the HO-1$^{+/-}$ group, which decreased to 119.3±11.7 mg/dl in the HO-1$^{+/-}$ + VCAM-1 antibody group ($P<0.05$, compared with the HO-1$^{+/-}$ group); at 72 h post-IRI, the BUN concentration value in the HO-1$^{+/-}$ group was 137.3±5.5 mg/dl, which decreased to 104.7±13.6 mg/dl in the HO-1$^{+/-}$ + VCAM-1 antibody animal group ($P<0.05$, compared with the HO-1$^{+/-}$ group). In addition, as shown in Fig. 3D, the SCr level in the HO-1$^{+/-}$ group at 24 h post-IRI was 1.56±0.13 mg/dl, which was decreased to 1.31±0.05 mg/dl in the HO-1$^{+/-}$ + VCAM-1 antibody group ($P<0.05$, compared with the HO-1$^{+/-}$ group). The SCr level in the HO-1$^{+/-}$ group at 72 h post-IRI was 1.32±0.04 mg/dl, which decreased to 1.13±0.04 mg/dl in the HO-1$^{+/-}$ + VCAM-1 antibody group ($P<0.05$, compared with the HO-1$^{+/-}$ group).

Cell death upon IRI measured by TUNEL assay. The numbers TUNEL-positive cells in the HO-1$^{+/-}$ group were evidently higher than those in the HO-1$^{+/+}$ group. However, in the HO-1$^{+/-}$ + VCAM-1 antibody group, the TUNEL-positive rate was significantly attenuated (Fig. 3E). Furthermore, the accumulation of macrophages (Fig. 3F) and neutrophils (Fig. 3G) was observed in the renal tubular area upon IRI, and this was more evident in the HO-1$^{+/-}$ group, as compared with the HO-1$^{+/+}$ group. However, in the HO-1$^{+/-}$ + VCAM-1 antibody group, leukocyte accumulation was significantly alleviated, indicating that HO-1 affects leukocyte recruitment and inflammatory injury at least partly through the VCAM-1 pathway.

In vitro blocking of VCAM-1 suppresses neutrophil adhesion and migration through Transwells. mGECs from the HO-1$^{+/-}$ knockdown and the wild-type mice were isolated, and following TNF-α stimulation, western blot analysis was used to identify the expression of HO-1 (Fig. 4A). A lower expression of HO-1 was observed in the HO-1$^{+/-}$ mGECs. However, higher expression levels of VCAM-1 were observed in the HO-1$^{+/-}$ mGECs than in the HO-1$^{+/+}$ mGECs by means of immunofluorescence staining. The fluorescence intensity of VCAM-1 expressed on the mGEC of the HO-1$^{+/-}$ mice was 2.04 times higher than that in the HO-1$^{+/+}$ control group (Fig. 4B). Neutrophil recruitment is an indispensable process of the immune response (34). Neutrophils were then isolated and labeled with PKH26 to perform adhesion assay and Transwell migration assay (Fig. 4C). As shown in Fig. 4D, the number of neutrophils adhered to the mGECs of the HO-1$^{+/-}$ mice was higher than that in the HO-1$^{+/+}$ group. However, when the VCAM-1 Ab were added to the culture medium, the number of neutrophils adhered to the mGECs was significantly reduced as compared with the HO-1$^{+/-}$ knockdown only group. In the Transwell migration assay, more neutrophils were observed migrating through the perforated membrane in the HO-1$^{+/-}$ group than in the HO-1$^{+/+}$ control group. However, when the VCAM-1 antibody was added to the culture medium, the number of migrating neutrophils was significantly reduced as compared with the HO-1$^{+/-}$ knockdown only group (Fig. 4E). These data suggest that HO-1 knockdown attenuated the adherence of neutrophils and their migration at least partly through the vascular basement membrane via VCAM-1.

Discussion

The present study demonstrates a protective role of HO-1 in renal IRI, leading to the following conclusions: i) HO-1 knockdown in HO-1$^{+/-}$ mice exacerbates renal IRI; ii) HO-1 knockdown aggravates renal IRI through the upregulation of VCAM-1 with a concomitant augmentation of leukocyte recruitment and inflammatory damage; iii) HO-1 knockdown increases neutrophil adherence and the migration of the vascular basement membrane *in vitro*, mediated by the upregulation of VCAM-1.

The protective effect of HO-1 on renal IRI has been widely recognized (35,36). Furthermore, HO-1 has been utilized as a therapeutic target for renal IRI. For example, Pannexin 1 silencing has been shown to attenuate renal IRI by inducing HO-1 expression (37). Hydrogen sulfide has also been shown to attenuates renal IRI by the upregulation of HO-1 (37). The results of the present study also demonstrated that HO-1 knockdown in HO-1$^{+/-}$ mice significantly exacerbated renal IRI with a concomitant increase in the serum levels of SCr and BUN markers, as well as the renal tubule injury score, which is consistent with the findings of previous studies (36,38,39).

HO-1 deficiency increases the infiltration of myeloid cells following IRI (37). The results of the present study demonstrated leukocyte accumulation in the renal tubular area following IRI, which included the accumulation of macrophages and neutrophils, that were more evident obvious in the HO-1$^{+/-}$ group than in the HO-1$^{+/+}$ control group. IRI is caused by the accumulation of neutrophils at the site of tissue injury and the release of a large number of inflammatory mediators, such as reactive oxygen species and cytokines. Neutrophil recruitment is a hallmark of an immune response, which is regulated by a cascade process, including cell roll, activation, adhesion and migration through the endothelium.

During this process, an essential role is played by very late antigen 4 (VLA-4) expressed on neutrophils binding to ICAM-1 and VCAM-1 expressed on the vascular endothelial cell surface (40,41). Therefore, the levels of VCAM-1 and ICAM-1 determine whether neutrophils can migrate through the endothelium. In the present study, VCAM-1 expression was significantly upregulated in the HO-$1^{+/-}$ mice as compared with the wild-type mice, which confirms that HO-1 inhibits the expression of VCAM-1.

To verify the effects of HO-1 on VCAM-1, VCAM-1 antibody was infused into HO-$1^{+/-}$ mice to block the endogenous pool of kidney VCAM-1. The results revealed that tubular injury was significantly reduced in the VCAM-1 antibody infusion group, exhibiting a decreased renal tubule injury score, BUN and SCr levels, and leukocyte recruitment, including neutrophils. This indicates that the effect of HO-1 knockdown requires the involvement of VCAM-1.

Leukocyte adhesion and migration to inflammatory sites through vascular endothelial cells are important features of the inflammatory processes accompanying IRI. The molecular basis of this process lies in the interaction between leukocytes and vascular endothelial cell surface adhesion factors, as well as in the regulation of the expression of adhesion molecules by cytokines and other factors. The effect of TNF-α on endothelial cells can lead to the upregulation of VCAM-1, leading to the increased adhesion of neutrophils to endothelial cells (40,42). The present study revealed markedly higher numbers of adhering and migrating neutrophils in the TNF-α treated HO-$1^{+/-}$ group than in the HO-$1^{+/+}$ control group, suggesting that the mGECs in the HO-$1^{+/-}$ group exhibited a higher VCAM-1 expression level, which was consistent with the results of western blot analysis. The anti-VCAM-1 antibody incubation experiments revealed that if the VCAM-1 on the mGEC surface in the $HO^{+/-}$ group was blocked, the number of adhering and migrating neutrophils significantly decreased, further indicating that the enhanced adhesive and migratory ability of neutrophils through mGECs in the HO-$1^{+/-}$ group was achieved by increasing VCAM-1 expression.

However, the present study has some limitations. Although it was demonstrated that HO-1 knockdown upregulated VCAM-1 expression to mediate neutrophil infiltration, it remains critical to further validate the detailed mechanisms through which HO-1 regulates VCAM-1 expression. Moreover, conditional HO-1 knockout models are also necessary for further validation.

In conclusion, the present study demonstrated that HO-1 knockdown in HO-$1^{+/-}$ mice exacerbated renal IRI via the upregulation of VCAM-1 with a concomitant augmentation of leukocyte recruitment and inflammatory damage. This, was further verified by neutrophil adherence and migration on a vascular basement membrane *in vitro*. The schematic diagram in presented Fig. 5 illustrates the mechanisms through which HO-1 protects against renal IRI injury proposed herein. These data thus suggest novel potential strategies for the clinical treatment of IR injury that typically follows renal transplantation.

Acknowledgements

Not applicable.

Funding

The present study was funded by the National Natural Science Foundation of China (grant no. 81801192) and by the Higher Educational Science and Technology Program of Shandong Province (grant no. J18KA141).

Availability of data and materials

The datasets used and/or analyzed during the current study are available from the corresponding author on reasonable request.

Authors' contributions

WB and YH conceived the study and established the initial design of the study. YH, HL, JY, HZ, YK and XL performed the experiments and analyzed the data. YH prepared the manuscript. WB and YH confirm the authenticity of all the raw data. All authors have read and approved the final manuscript.

Ethics approval and consent to participate

All experiments performed in the present study were approved by the Institutional Animal Care and Use Committee of Binzhou Medical University (PJ2018-10-16).

Patient consent for publication

Not applicable.

Competing interests

The authors declare that they have no competing interests.

References

1. Dong Y, Zhang Q, Wen J, Chen T, He L, Wang Y, Yin J, Wu R, Xue R, Li S, *et al*: Ischemic duration and frequency determines AKI-to-CKD progression monitored by dynamic changes of tubular biomarkers in IRI mice. Front Physiol 10: 153, 2019.
2. Sheashaa H, Lotfy A, Elhusseini F, Aziz AA, Baiomy A, Awad S, Alsayed A, El-Gilany AH, Saad MA, Mahmoud K, *et al*: Protective effect of adipose-derived mesenchymal stem cells against acute kidney injury induced by ischemia-reperfusion in Sprague-Dawley rats. Exp Ther Med 11: 1573-1580, 2016.
3. Cheng Q and Wang L: LncRNA XIST serves as a ceRNA to regulate the expression of ASF1A, BRWD1M, and PFKFB2 in kidney transplant acute kidney injury via sponging hsa-miR-212-3p and hsa-miR-122-5p. Cell Cycle 19: 290-299, 2020.
4. Yang C, Qi R and Yang B: Pathogenesis of chronic allograft dysfunction progress to renal fibrosis. Adv Exp Med Biol 1165: 101-116, 2019.
5. Zhang A, Wan B, Jiang D, Wu Y, Ji P, Du Y and Zhang G: The cytoprotective enzyme heme oxygenase-1 suppresses pseudorabies virus replication in vitro. Front Microbiol 11: 412, 2020.
6. Haines DD and Tosaki A: Role of heme oxygenases in cardiovascular syndromes and co-morbidities. Curr Pharm Des 24: 2322-2325, 2018.
7. Sun XQ, Wu C, Qiu YB, Wu YX, Chen JL, Huang JF, Chen D and Pang QF: Heme oxygenase-1 attenuates seawater drowning-induced acute lung injury through a reduction in inflammation and oxidative stress. Int Immunopharmacol 74: 105634, 2019.
8. Xu X, He X, Liu J, Qin J, Ye J and Fan M: Protective effects of hydrogen-rich saline against renal ischemia-reperfusion injury by increased expression of heme oxygenase-1 in aged rats. Int J Clin Exp Pathol 12: 1488-1496, 2019.

9. Seo MS, Kim HJ, Kim H and Park SW: Ethyl pyruvate directly attenuates active secretion of HMGB1 in proximal tubular cells via induction of heme oxygenase-1. J Clin Med 8: 629, 2019.
10. Barakat M, Gabr MM, Zhran F, El-Adl M, Hussein AM, Barakat N and Eldemerdash R: Upregulation of heme oxygenase 1 (HO-1) attenuates kidney damage, oxidative stress and inflammatory reaction during renal ischemia/reperfusion injury. Gen Physiol Biophys 37: 193-204, 2018.
11. Baan C, Peeters A, Lemos F, Uitterlinden A, Doxiadis I, Claas F, Ijzermans J, Roodnat J and Weimar W: Fundamental role for HO-1 in the self-protection of renal allografts. Am J Transplant 4: 811-818, 2004.
12. Rund KM, Peng S, Greite R, Claassen C, Nolte F, Oger C, Galano JM, Balas L, Durand T, Chen R, *et al*: Dietary omega-3 PUFA improved tubular function after ischemia induced acute kidney injury in mice but did not attenuate impairment of renal function. Prostaglandins Other Lipid Mediat 146: 106386, 2020.
13. Wadey RM, Connolly KD, Mathew D, Walters G, Rees DA and James PE: Inflammatory adipocyte-derived extracellular vesicles promote leukocyte attachment to vascular endothelial cells. Atherosclerosis 283: 19-27, 2019.
14. Coenen DM, Mastenbroek TG and Cosemans J: Platelet interaction with activated endothelium: Mechanistic insights from microfluidics. Blood 130: 2819-2828, 2017.
15. Cheng Q, McKeown SJ, Santos L, Santiago FS, Khachigian LM, Morand EF and Hickey MJ: Macrophage migration inhibitory factor increases leukocyte-endothelial interactions in human endothelial cells via promotion of expression of adhesion molecules. J Immunol 185: 1238-1247, 2010.
16. Ma YR and Ma YH: MIP-1α enhances jurkat cell transendothelial migration by up-regulating endothelial adhesion molecules VCAM-1 and ICAM-1. Leuk Res 38: 1327-1331, 2014.
17. Sumagin R, Lomakina E and Sarelius IH: Leukocyte-endothelial cell interactions are linked to vascular permeability via ICAM-1-mediated signaling. Am J Physiol Heart Circ Physiol 295: H969-H977, 2008.
18. Jung TW, Park HS, Jeong JH and Lee T: Salsalate ameliorates the atherosclerotic response through HO-1- and SIRT1-mediated suppression of ER stress and inflammation. Inflamm Res 68: 655-663, 2019.
19. Pérez S, Pereda J, Sabater L and Sastre J: Pancreatic ascites hemoglobin contributes to the systemic response in acute pancreatitis. Free Radic Biol Med 81: 145-155, 2015.
20. Vinchi F, Gastaldi S, Silengo L, Altruda F and Tolosano E: Hemopexin prevents endothelial damage and liver congestion in a mouse model of heme overload. Am J Pathol 173: 289-299, 2008.
21. Hassan M, Bakar NS, Aziz MA, Basah NK and Singh HJ: Leptin-induced increase in blood pressure and markers of endothelial activation during pregnancy in Sprague Dawley rats is prevented by resibufogenin, a marinobufagenin antagonist. Reprod Biol 20: 184-190, 2020.
22. Li H, Peng W, Jian W, Li Y, Li Q, Li W and Xu Y: ROCK inhibitor fasudil attenuated high glucose-induced MCP-1 and VCAM-1 expression and monocyte-endothelial cell adhesion. Cardiovasc Diabetol 11: 65, 2012.
23. Chakraborty S, Hu SY, Wu SH, Karmenyan A and Chiou A: The interaction affinity between vascular cell adhesion molecule-1 (VCAM-1) and very late antigen-4 (VLA-4) analyzed by quantitative FRET. PLoS One 10: e121399, 2015.
24. Hart R and Greaves DR: Chemerin contributes to inflammation by promoting macrophage adhesion to VCAM-1 and fibronectin through clustering of VLA-4 and VLA-5. J Immunol 185: 3728-3739, 2010.
25. Cao YA, Wagers AJ, Karsunky H, Zhao H, Reeves R, Wong RJ, Stevenson DK, Weissman IL and Contag CH: Heme oxygenase-1 deficiency leads to disrupted response to acute stress in stem cells and progenitors. Blood 112: 4494-4502, 2008.
26. Park JG, Ryu SY, Jung IH, Lee YH, Kang KJ, Lee MR, Lee MN, Sonn SK, Lee JH, Lee H, *et al*: Evaluation of VCAM-1 antibodies as therapeutic agent for atherosclerosis in apolipoprotein E-deficient mice. Atherosclerosis 226: 356-363, 2013.
27. Kucherenko MM, Marrone AK, Rishko VM, Yatsenko AS, Klepzig A and Shcherbata HR: Paraffin-embedded and frozen sections of Drosophila adult muscles. J Vis Exp 27: 2438, 2010.
28. Chen CB, Liu LS, Zhou J, Wang XP, Han M, Jiao XY, He XS and Yuan XP: Up-regulation of HMGB1 exacerbates renal ischemia-reperfusion injury by stimulating inflammatory and immune responses through the TLR4 signaling pathway in mice. Cell Physiol Biochem 41: 2447-2460, 2017.
29. Ellis JL and Yin C: Histological analyses of acute alcoholic liver injury in zebrafish. J Vis Exp 25: 55630, 2017.
30. Tanaka S, Tanaka T, Kawakami T, Takano H, Sugahara M, Saito H, Higashijima Y, Yamaguchi J, Inagi R and Nangaku M: Vascular adhesion protein-1 enhances neutrophil infiltration by generation of hydrogen peroxide in renal ischemia/reperfusion injury. Kidney Int 92: 154-164, 2017.
31. Garcia-Cenador MB, Lorenzo-Gomez MF, Herrero-Payo JJ, Ruiz J, de Obanos MP, Pascual J, Lopez-Novoa JM and Garcia-Criado FJ: Cardiotrophin-1 administration protects from ischemia-reperfusion renal injury and inflammation. Transplantation 96: 1034-1042, 2013.
32. Livak KJ and Schmittgen TD: Analysis of relative gene expression data using real-time quantitative PCR and the 2(-Delta Delta C(T)) method. Methods 25: 402-408, 2001.
33. Cui A, Xiang M, Xu M, Lu P, Wang S, Zou Y, Qiao K, Jin C, Li Y, Lu M, *et al*: VCAM-1-mediated neutrophil infiltration exacerbates ambient fine particle-induced lung injury. Toxicol Lett 302: 60-74, 2019.
34. Block H, Herter JM, Rossaint J, Stadtmann A, Kliche S, Lowell CA and Zarbock A: Crucial role of SLP-76 and ADAP for neutrophil recruitment in mouse kidney ischemia-reperfusion injury. J Exp Med 209: 407-421, 2012.
35. Rossi M, Delbauve S, Roumeguère T, Wespes E, Leo O, Flamand V, Moine AL and Hougardy JM: HO-1 mitigates acute kidney injury and subsequent kidney-lung cross-talk. Free Radic Res 53: 1035-1043, 2019.
36. Rossi M, Thierry A, Delbauve S, Preyat N, Soares MP, Roumeguère T, Leo O, Flamand V, Moine AL and Hougardy JM: Specific expression of heme oxygenase-1 by myeloid cells modulates renal ischemia-reperfusion injury. Sci Rep 7: 197, 2017.
37. Su L, Jiang X, Yang C, Zhang J, Chen B, Li Y, Yao S, Xie Q, Gomez H, Murugan R and Peng Z: Pannexin 1 mediates ferroptosis that contributes to renal ischemia/reperfusion injury. J Biol Chem 294: 19395-19404, 2019.
38. Ferenbach DA, Ramdas V, Spencer N, Marson L, Anegon I, Hughes J and Kluth DC: Macrophages expressing heme oxygenase-1 improve renal function in ischemia/reperfusion injury. Mol Ther 18: 1706-1713, 2010.
39. Ding M, Tolbert E, Birkenbach M, Akhlaghi F, Gohh R and Ghonem NS: Treprostinil, a prostacyclin analog, ameliorates renal ischemia-reperfusion injury: Preclinical studies in a rat model of acute kidney injury. Nephrol Dial Transplant 36: 257-266, 2021.
40. Buffone AJ, Anderson NR and Hammer DA: Human neutrophils will crawl upstream on ICAM-1 If Mac-1 is blocked. Biophys J 117: 1393-1404, 2019.
41. Chen WC, Chen NJ, Chen HP, Yu WK, Su VYF, Chen H, Wu HH and Yang KY: Nintedanib reduces neutrophil chemotaxis via activating GRK2 in bleomycin-induced pulmonary fibrosis. Int J Mol Sci 21: 4735, 2020.
42. Taubitz A, Schwarz M, Eltrich N, Lindenmeyer MT and Vielhauer V: Distinct contributions of TNF receptor 1 and 2 to TNF-induced glomerular inflammation in mice. PLoS One 8: e68167, 2013.